Fabrication of a Micro-omnifluidic Device by Omniphilic/Omniphobic Patterning on Nanostructured Surfaces

Inseong You,[†] Tae Geol Lee,[‡] Yoon Sung Nam,[§,∥] and Haeshin Lee*[,†,∥,⊥]

[†]Graduate School of Nanoscience & Technology, Korea Advanced Institute of Science and Techology, Daejeon 305-701, Republic of Korea, [‡]Center for Nano-Bio Technology, Korea Research Institute of Standards and Science, Daejeon 305-600, Republic of Korea, and [§]Department of Materials Science and Engineering, [∥]Center for Nature-inspired Techology (CNiT) in KAIST Institute NanoCentury (KINC), and [⊥]Department of Chemistry, Korea Advanced Institute of Science and Techology, Daejeon 305-701, Republic of Korea

ABSTRACT We integrate the adhesive properties of marine mussels, the lubricating properties of pitcher plants, and the nonfouling properties of diatoms into nanostructured surfaces to develop a device called a micro-omnifluidic (μ-OF) system to solve the existing challenges in microfluidic systems. Unlike conventional poly(dimethylsiloxane)-based fluidic systems that are incompatible with most organic solvents, the μ-OF system utilizes a variety of solvents such as water, ethanol, dimethyl sulfoxide, dimethylformamide, tetrahydrofuran, *n*-hexane, 1,2-dichloroethane, acetic acid, 2-propanol, acetone, toluene, diesel oil, dioxane, gasoline oil, hexadecane, and xylene. The μ-OF system is based on a phenomenon called microchannel induction that spontaneously occurs when virtually all droplets of solvents are applied on omniphilically micropatterned regions of a slippery liquid-infused porous surface. Any solvents with surface tension greater than that of the lubricant (17.1 mN/m, Fluorinert FC-70) are able to repel the infused lubricant located on top of the omniphilic microlines, triggering controlled movement of the droplet by gravity along the microlines. We also demonstrated that the μ-OF system is reusable by the nonadsorption properties of the silicified layer. Due to the organic solvent compatibility, we were able to perform organic reactions with high portability and energy efficiency in operation.

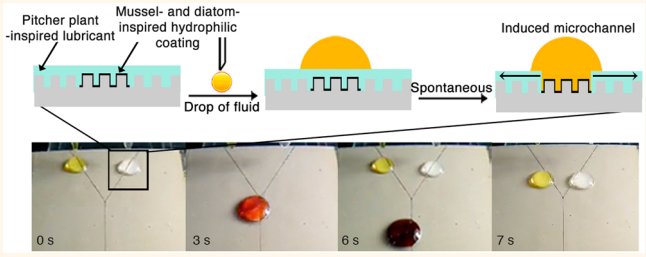

KEYWORDS: nature-inspired · microfluidics · mussels · diatoms · pitcher plants · organic solvents

Over the past two decades, three-dimensional (3D) microfluidic devices have replaced a variety of laboratory devices due to the abilities to utilize minute quantities of samples and to perform separations, detections, and analysis with high sensitivity, with low cost, and in short times.[1] The 3D microfluidic devices have been widely used for biological and chemical assays,[1−5] confined reactions,[6,7] drug screening,[8] and microenvironmental modeling of human tissues.[9−11] Considering that poly(dimethylsiloxane) (PDMS) microchannels are widely implemented worldwide, one critical issue is the incompatibility of PDMS to organic solvents, which severely limits the utility of microfluidic systems. For example, Whitesides' group demonstrated that solvents such as benzene, hexane, xylene, chloroform, and tetrahydrofuran (THF) are incompatible with PDMS because of swelling.[12] Furthermore, the enhancement of portability and reusability is beneficial for practical utility in applications such as bio/chemical assays.

Recently, surface-tension-confined microfluidic (STCM) devices operate as mostly 2D platforms. In those devices, small volumes of liquid droplets are confined to the specific surface area exhibiting high surface energy with low surface energy background. The use of STCM devices solves the portability issues by self-driving or guiding liquids through surface tension gradients, capillary force, and gravitational force.[13−17] Also, as the device is exposed to external environments, introduction of sample liquid is very easy. Thus, the STCM devices have been applied to practical applications such as urine analysis (protein, glucose, or pH detection), immunoassays/ELISA, and synthesis of metal nanoparticles.[13] However, other challenges, such as organic solvent compatibility and fouling problems, remain

* Address correspondence to haeshin@kaist.ac.kr.

Received for review April 23, 2014 and accepted September 4, 2014.

Published online September 04, 2014
10.1021/nn502226v

unsolved due to the difficulty of creating a lithographic omniphilic pattern (*i.e.*, a low contact angle upon exposure to both organic solvents and water) on omniphobic background surfaces. In addition, the simultaneous realization of both omniphilic and omniphobic properties with the same surface is also difficult.

Here, we report a new concept called a micro-omnifluidic device (μ-OF). Lithographic micropatterns inspired by the chemistry of mussels and diatoms exhibiting omniphilic properties were fabricated on an omniphobic background that is prepared by infusion of a *Nepenthes* pitcher plant-inspired lubricant in the nanostructured surfaces. The mussel- and diatom-inspired poly(dopamine) approaches were adapted from our previous studies,[18−22] and the pitcher plant-inspired approach was adapted from the studies by Aizenberg's group.[23−25] As expected, the fabricated μ-OF device is compatible with a variety of solvents such as water, ethanol, dimethyl sulfoxide (DMSO), dimethylformamide (DMF), tetrahydrofuran (THF), *n*-hexane, 1,2-dichloroethane, acetic acid, 2-propanol, acetone, toluene, diesel oil, dioxane, gasoline oil, hexadecane, and xylene. The μ-OF system is based on a new phenomenon called microchannel induction on surfaces that spontaneously occurs when virtually all droplets of solvents are applied on the omniphilically patterned region of a slippery liquid-infused porous surface (SLIPS). Any solvents with surface tension greater than that of the lubricant (17.1 mN/m, Fluorinert FC-70) are able to repel the infused lubricant located on top of the omniphilic microlines, triggering controlled movement of the droplet by gravity along the omniphilic microlines. The microchannel induction is an energetically favorable phenomenon explained by the total change in interfacial energy at equilibrium. The μ-OF system is reusable by the nonadsorption properties of the silicified layer. Due to the organic solvent compatibility, organic reactions on microchannels were able to be performed with high portability and energy efficiency in operation. The μ-OF system described herein is a step toward an ideal fluidic device for many potential applications.

RESULTS AND DISCUSSION

Microchannel-Inducible Slippery Liquid-Infused Porous Surface (mi-SLIPS). The most challenging part of successfully creating μ-OF devices is preparing appropriate surfaces. In principle, an omniphobic surface is first required because nearly all solvents, including water, should roll on the surface *via* gravitational force. Additionally, an omniphilic microline is necessary to act as a solvent-guiding pathway. To prepare the omniphobic surface, we were inspired by the liquid-repelling mechanism of the *Nepenthes* pitcher plant. This plant has a tube-shaped trap with an inner surface consisting of a slippery aqueous solution and slanted, hairy microcellulose.[26−28] In addition, we were inspired by the solvent-resistant adhesion mechanism of marine mussels, which plays an important role in creating highly adhesive interfaces.[18,19] A poly(dopamine) coating was formed on an aluminum surface *via* the oxidative polymerization of dopamine hydrochloride (first step, Figure 1a).[18] The appearance of the N 1s photoelectron peak and the disappearance of the Al 2p peak in the spectrum of X-ray photoelectron spectroscopy (XPS) confirmed that poly(dopamine) with a thickness of over 10 nm was successfully formed (Figure 1b, top). The exact thickness of the poly(dopamine) was 20 $\pm$ 2 nm, confirmed by the elipsometer analysis. The root-mean-square (rms) roughness of the poly(dopamine) coating measured by atomic force microscopy (AFM) was 1.5 nm (Figure 1c, top). This poly(dopamine) layer initiated a sol−gel reaction to form a 1 μm thick TiO_2 adlayer from a titanium(IV) isopropoxide precursor (second step, Figure 1a and Supporting Information Figure S1). The appearance of the Ti 2p peak in the XPS spectrum confirmed the formation of a TiO_2 layer (Figure 1b, second from top). The rms roughness of the formed TiO_2 layer was 219.3 nm (Figure 1c, bottom). Subsequently, the surface was immersed into a fluorophosphate surfactant solution, zonylFSE, for the fluorination of the surface (third step, Figure 1a).[20] The appearance of the F 1s peak in the XPS spectrum confirmed the fluorination (Figure 1b, third from top). To create a two-dimensional omniphilic path, photolithography was performed using a positive photoresist (AZ5214) (fourth and fifth step, Figure 1a). After development (MIF-300), the one-pot poly(dopamine) coating method was performed over 5 h to immobilize 2-dimethylaminoethanethiol on the surface *in situ* during the poly(dopamine) formation. The tertiary amine in the 2-dimethylaminoethanethiol triggers a biosilicification reaction that forms a nanothin silica layer (sixth step, Figure 1a).[21,22] The appearance of Si 2s and Si 2p peaks and the disappearance of the F 1s peak in the XPS spectrum confirmed the silicification, and the existence of Ti 2p indicated that the thickness of the silica coating layer was less than 10 nm (Figure 1b, bottom). Finally, the lubricant solution, Fluorinert FC-70, was added to the entire surface. Fluoinert FC-70 was known to be nonvolatile, immiscible with both aqueous and hydrocarbon phases, and capable of stably forming a slippery film with solid substrates for a variety of polar and nonpolar liquids.[23,24] The rough nanoscale surfaces allowed for the spontaneous infusion of the lubricant and maintained stability (seventh step, Figure 1a). The thickness of the lubricant was 30 $\pm$ 3 μm, measured by a conforcal microscope (Supporting Information Figure S2).

The background surface exhibited unique liquid-repelling properties previously known as a SLIPS.[23−25] In the SLIPS region, all tested solvents including water, ethanol, DMSO, DMF, THF, *n*-hexane, 1,2-dichloroethane, acetic acid, 2-propanol, acetone, toluene, diesel oil, dioxane, gasoline oil, hexadecane, and xylene were

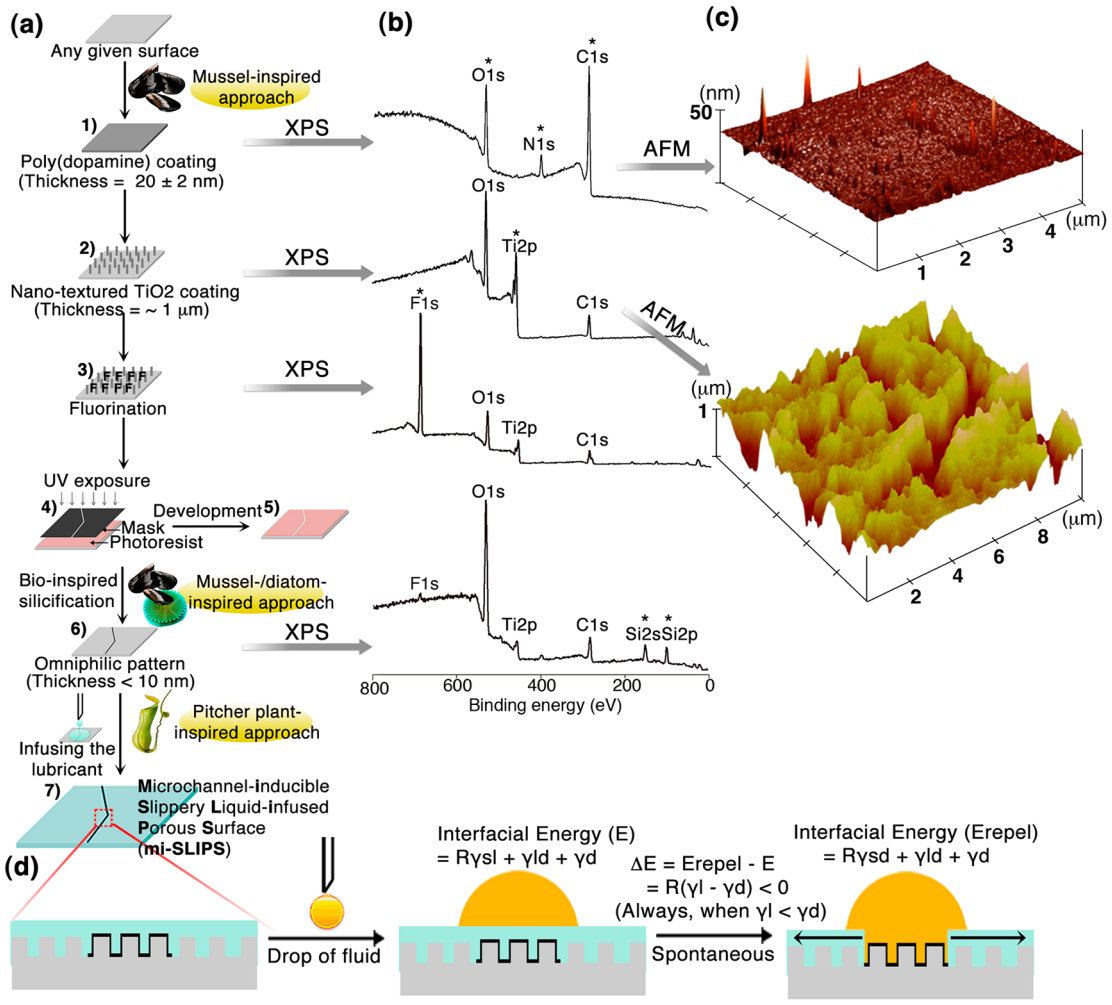

Figure 1. Fabrication of mi-SLIPS. (a) Schematic for the fabrication procedure of mi-SLIPS. Mussel-, diatom-, and pitcher plant-inspired approaches were utilized. (b) Survey XPS spectra corresponding to the poly(dopamine)-coated (first from the top), the TiO_2-coated (second), the fluorinated (third), and the silicified (fourth) surfaces. (c) AFM images of the poly(dopamine)-coated (top) and the TiO_2-coated (bottom) surfaces. (d) Schematic explanation of the displacement of the lubricant on the silicified area by a droplet of solvent on top.

successfully repelled. The solvent repellency resulted in the low contact angle hysteresis ($\Delta\theta$) of 2° in the process of droplet sliding and the low sliding angle under 5° (Figure 2a and Supporting Information Figure S3). Although the lubricant ubiquitously formed the topmost layer (Figure 1d, left), interactions between the lubricant and fluorinated solid in the SLIPS and between the lubricant and silicified solid should differ significantly. We hypothesized that the lubricant, which is a stable SLIPS, can be displaced by the introduction of a solvent droplet. In other words, the lubricant itself is repelled by the incoming solvents. We tested this hypothesis by comparing the thermodynamic energies at the interfaces. The first consideration is the three-layered structure consisting of the silicified surface (bottom), lubricant (middle), and solvent droplet (top). In this case, the interfacial energy (E) is defined by $R\gamma_{sl} + \gamma_{ld} + \gamma_{d}$, where γ_{sl} is the interfacial energy between the silicified surface and lubricant, γ_{ld} is the energy between the lubricant and solvent, and γ_{d} is the energy between the solvent and air. Finally, R is the roughness factor. Likewise, we considered a second case, a two-layer structure, where the applied solvent droplet repels the lubricant. In this case, the energy (E_{repel}) is defined by $R\gamma_{sd} + \gamma_{ld} + \gamma_{d}$, where γ_{sd} is the energy between the silicified surface and solvent. When we subtract E from E_{repel} ($\Delta E = E_{repel} - E$), the resultant energy equation is as follows:

$$\Delta E = R(\gamma_l \cos\theta_l - \gamma_d \cos\theta_d) \quad (1)$$

where γ_l is the lubricant surface tension, θ_l and θ_d are the equilibrium contact angles of the lubricant and solvent on a flat silicified solid surface, respectively. For a flat silicified surface, the solvent and lubricant contact angles approach 0° (Supporting Information Figure S4). Thus, eq 1 above can be simplified as follows:

$$\Delta E = R(\gamma_l - \gamma_d) \quad (2)$$

Equation 2 predicts that if γ_d is greater than γ_l (17.1 mN/m), the sign of ΔE is always negative (<0).

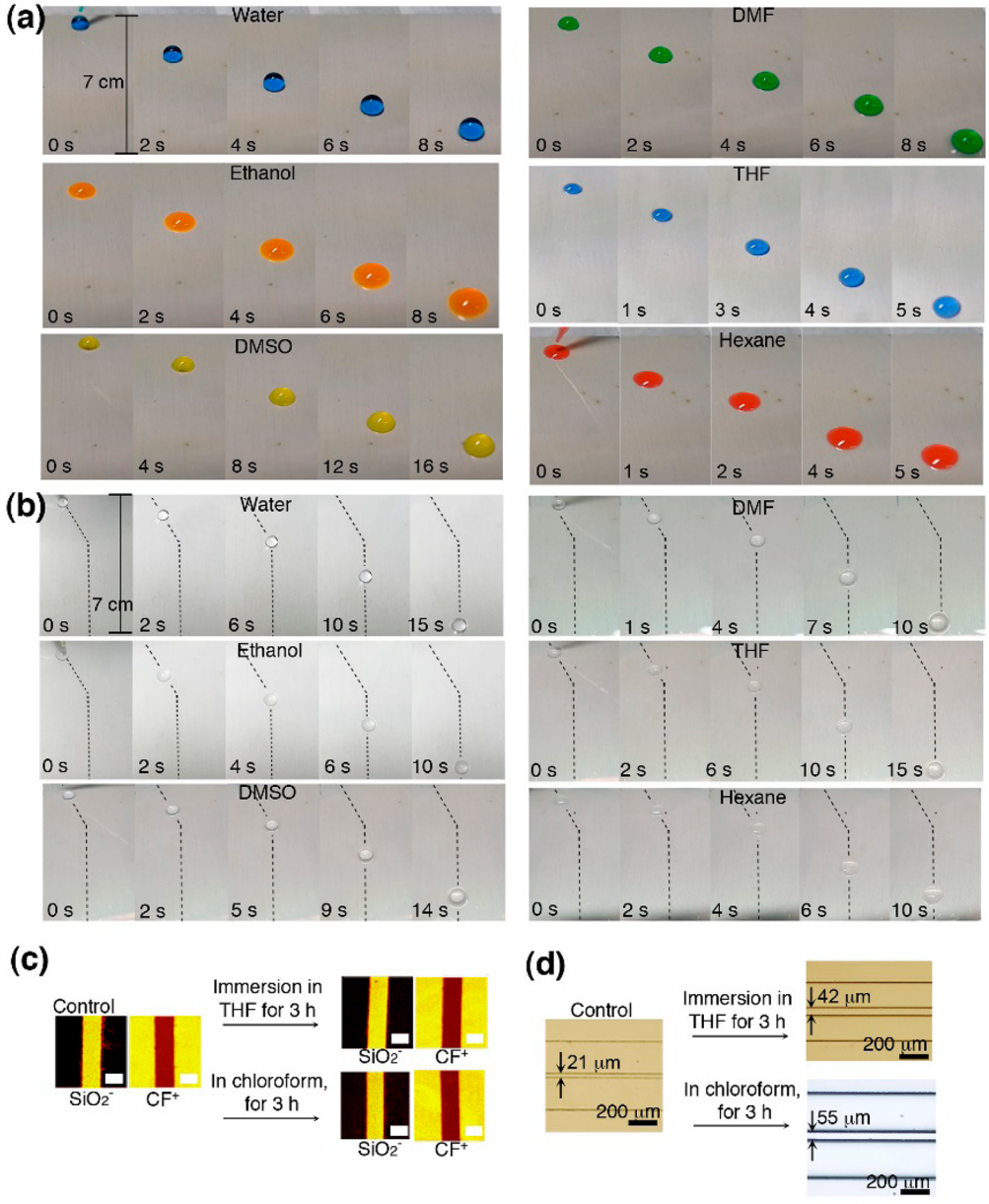

Figure 2. Characterization of the microchannels prepared by the mi-SLIPS method. (a,b) Experiments to test solvent compatibility on the SLIPS surfaces (water, ethanol, DMSO, DMF, THF, and hexane, 20 μL) (a) and on the induced kinked microchannel of the mi-SLIPS surfaces for prototype of the Y-shaped mixing device (the droplet volume of 10 μL) (b) that is demonstrated in Figure 3. (c) ToF-SIMS images of the induced microlines of the mi-SLIPS before (control) and after immersion in the THF and chloroform solvents: SiO_2^- ion signal for the microchannel (left) and CF^+ ion for omniphobic background (right). The scale bar is 60 μm. (d) Model PDMS microfluidic channels were immersed in the THF and chloroform solvents for 3 h, which exhibited significant swelling, indicating incompatibility.

Therefore, an important conclusion predicts "spontaneous displacement of the lubricant" when a solvent is applied (Figure 1d, middle and right). This conclusion predicts that the fabricated microlines act as solvent-guiding pathways because of spontaneous lubricant displacement. In other words, two-dimensional channels are induced by simply dropping a solvent onto the fabricated microlines. We named this process microchannel-inducible slippery liquid-infused porous surface.

In fact, this concept was experimentally realized (Figure 2b). A microchannel was indeed induced upon solvent introduction to the silicified microline regardless of the solvent type (water, ethanol, DMSO, DMF, THF, and *n*-hexane) (the microline width = 60 μm), and as predicted, the solvent droplet slowly moved down the induced kinked microchannel due to gravity (slope angle = 5°). The speed of the spontaneous lubricant displacement was measured by depositing droplets of different solvents (water, DMSO, THF, and ethanol; mass = 10 μg) on the silicified TiO_2 surface and recording the time when the displacement was initiated by a high-speed camera (60 frames/1 s).

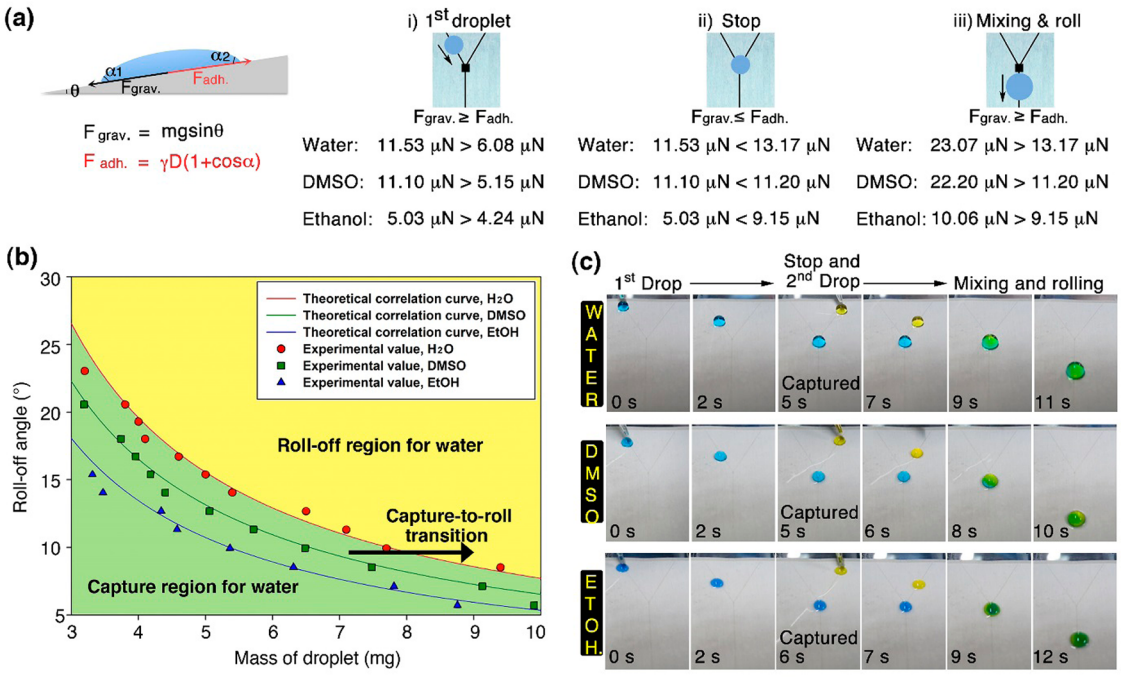

Figure 3. (a) Micro-omnifluidic device and explanation of the operational principles using the force balance equation. We defined the downward (F_{grav}) and upward (F_{adh}) components, and each equation is described in the figure and text. Based on its mass and surface tension, a solvent droplet rolls downward, is captured to wait for the second droplet, and rolls down again after merging. At each rolling and capture step, the magnitude of the force alternates ($F_{grav} > F_{adh}$ (i), $F_{grav} < F_{adh}$ (ii), and $F_{grav} > F_{adh}$ (iii)). A detailed calculation is shown in Table S1. (b) Theoretical prediction (red line for water, green for DMSO, and blue for ethanol) and experimental confirmation of the roll-off angle and droplet mass relationship (red dots for water, green for DMSO, and blue for ethanol). The roll-off angle is the surface slope angle at which the droplet starts to roll down the surface. For example, increasing the mass by merging two droplets transitions from captured to rolling (indicated by the arrow). (c) Demonstration of microfluidic mixing using the μ-OF device. As predicted in panel (b), the droplet movement was precisely controlled by the micropatch. The first droplet was captured on the micropatch (first and second photos). When the second droplet was added (third to fifth photos), the resulting mixed droplet moved downward (sixth photo). The droplet volumes and tilt angles are as follows: 8.0 μL and 8.5° (water), 7.0 μL and 8.5° (DMSO), and 5.1 μL and 7.1° (ethanol).

As a result, the displacement did not happen immediately but started after 150 ms for the water droplet, 135 ms for DMSO, 120 ms for THF, and 120 ms for ethanol (avg = 130 ± 13 ms), which demonstrates that the displacement kinetics was varied depending on the chemical structure of solvent (thickness = 30 ± 3 μm) (Supporting Information Figure S5). The stability of the silicified microline was tested by immersing the lubricant-infused mi-SLIPS substrates into THF (Figure 2c, top) and chloroform (Figure 2c, bottom) for 3 h. Then, the mi-SLIPS substrates were analyzed *via* time-of-flight secondary ion mass spectrometry (ToF-SIMS). The strong SiO_2^- fragment (m/z = 60) from the silicified area and CF^+ fragment (m/z = 31) from the lubricant-infused area detected before the solvent immersion (Figure 2c, left) were completely unchanged after the solvent immersion (Figure 2c, right). The detection of silicon and fluorine in the ToF-SIMS analysis was consistent with the XPS results, where the Si 2s, Si 2p, and F 1s photoelectron peaks were observed (Figure 1b, bottom). The silicified microlines also remained stable in other organic solvents, including ethanol, methanol, dioxane, DMSO, and toluene (Supporting Information Figure S6). However, conventional PDMS-based microchannels were incompatible with THF and chloroform because of significant swelling.[12] When the PDMS microchannels were immersed in THF or chloroform for 3 h, the resultant swelling enlarged the microchannels and caused a malfunction in the microfluidic device (Figure 2d). This solvent-resistant property for the mi-SLIPS-based devices can be useful for organic solvent mixing devices.

Designing a Micro-omnifluidic Device. The mi-SLIPS is an important principle used in Y-patterned droplet mixing devices (microline width = 60 μm) with large, omniphilic, square micropatches ($x = y$ = 200 μm) at the mixing point. The patterned surface placement at a slope angle from 7 to 9° applied a gravitational force to the droplets, as shown in Figure 3a. The first droplet was introduced at either of the two Y-shaped microline inlets and subsequently captured at the micropatch to wait for the second droplet. When the second droplet mixes with the first one, the increased weight causes the droplets to roll, which facilitates mixing. Unlike PDMS-based microfluidic systems that use syringe pumps, this device requires no pump and is compatible with almost any solvent, including water, DMSO, and ethanol, as demonstrated in Figure 2. Thus, we named this type of a device a "micro-omnifluidic system".

An important feature of the μ-OF system is the square omniphilic micropatch at the microline intersection. This patch creates enough surface energy to capture the first droplet but not enough to hold the droplets after the second droplet is mixed. Thus, the micropatch acts as a microvalve in a conventional PDMS microfluidic device.

The gravitational force (F_{grav}) acting on the droplet can be described as $F_{grav} = mg \sin \theta$, where m is the droplet mass, g is the gravitational acceleration (9.81 m/s^2), and θ is the surface tilting angle (*i.e.*, slope angle). The adhesion force (F_{adh}) can be expressed using the Young and Dupré equation.[29,30]

$$F_{adh} = \gamma_L D(1 + \cos \alpha) \quad (3)$$

where γ_L is the surface tension of the liquid droplet, D is the perimeter length created by the liquid/surface contact, and α is the static contact angle for the test liquid. A comparison of the experimentally measured F_{grav} and F_{adh} for the test liquid (water, DMSO, and ethanol) is summarized (Supporting Information Table S1). When the first droplet was placed on the μ-OF device microline (part i, Figure 3a), F_{grav} was 11.53 μN for water, 11.10 μN for DMSO, and 5.03 μN for ethanol, which was larger than the adhesion forces (F_{adh}) for water (6.08 μN), DMSO (5.15 μN), and ethanol (4.24 μN), resulting in the droplet rolling. When the first liquid reached the square micropatch (part ii, Figure 3a), the force magnitudes reversed, $F_{grav} < F_{adh}$. F_{grav} was unchanged; however, F_{adh} for water, DMSO, and ethanol increased to 13.17, 11.20, and 9.15 μN, respectively, as the perimeter, D, in eq 3 increased at the micropatch. In this situation, the droplet stops at the patch. Finally, when the second droplet mixed with the captured one (part iii, Figure 3a), F_{adh} remained unchanged, but F_{grav} increased due to the mass increase (23.07 μN for water, 22.20 μN for DMSO, and 10.06 μN for ethanol). In this situation, the captured droplet begins to roll again.

Another important μ-OF device variable is the slope angle (*i.e.*, tilting angle). The roll-off angle (θ) is the minimum angle required for the captured droplet to roll off from the micropatch, as determined by $F_{adh} = F_{grav}$:

$$\theta = \sin^{-1}(\gamma_L D/mg(1 + \cos \alpha)) \quad (4)$$

Equation 4 shows that the roll-off angle is a function of the droplet mass and surface tension. Mathematically, for a given droplet mass, the roll-off angle decreased in order of water (red line) to DMSO (green) to EtOH (blue). This order corresponds to the liquid surface tensions (Figure 3b). For a given solvent, θ should increase as m decreases. For all three cases, water, DMSO, and ethanol, the theoretical calculations and experimental data correlated well, indicating that eq 4 is reliable. As expected, the first water droplet (8.0 μL, blue) was captured by a μ-OF device with a slope angle of 8.5° and waited for the second droplet (Figure 3c, first row). When the second droplet was introduced (8.0 μL, yellow) and subsequently mixed, the droplet color rapidly turned green. At the same time, the mixed droplet started to move downward. This capture-to-roll transition induced by the increased mass is also explained in Figure 3b (arrow). This capture-to-roll experiment was also performed using stained DMSO and ethanol droplets under different conditions to confirm the aforementioned prediction (DMSO: 7.0 μL (vol), 8.5° (tilting angle); ethanol: 5.1 μL, 7.1°). The results correlate well with the prediction.

Reusabillity Test of the μ-OF Device. Surface fouling (*i.e.*, adsorption) by dissolved components in the flow has been a problem in PDMS-based fluidic systems.[31,32] Fouling significantly decreases the device reusability and biases some quantification results. To test for surface fouling in the μ-OF device, we performed experiments using fluorescent dye solutions, Hoechst 33342 (soluble in water; λ_{exc} (nm) = 350, λ_{em} = 461) and fluorescein isothiocyanate (FITC) (soluble in ethanol; λ_{exc} = 490, λ_{em} = 525). After the μ-OF device was immersed in an aqueous Hoechst 33342 solution (2 mg/mL) for 1 min, a blue fluorescence appeared in the 60 μm wide microchannel. To remove the fouled Hoechst 33342, the μ-OF device was immersed in DI water and sonicated for 10 min (50 kHz, 150 W). Afterward, the blue fluorescence had completely disappeared, which indicates that the fouled dye was detached (Figure 4a, top row). The cleaned μ-OF device was then immersed in an FITC ethanol solution (2 mg/mL) for 1 min. As expected, a green fluorescence appeared in the microchannel and subsequently disappeared after sonication (Figure 4a, bottom row). After each washing step, the μ-OF device was not required to be relubricated due to the immiscibility of the FC-70 lubricant infused in the fluorinated rough surface with solvents including water. Thus, the μ-OF device could be repeatedly used by simply washing with ultrasonication. In particular, the variety of solvents compatible with μ-OF devices can all be utilized for this washing process.

Three-Dimensional, Multilayered μ-OF Device. One important advantage of μ-OF devices is their capabilities with multilayered configurations (Figure 4b). Such a configuration provides the device with several unprecedented possibilities. First, the running time can be increased dramatically. Figure 4b shows that the running time was easily increased beyond 1 min. This long running time is an important advantage in some applications such as chemical reactions and bioassays because a complete reaction of two different reagents in a droplet can be achieved simply by rolling the droplet for the long time scale. The running time of the conventional microfluidic devices is between 1 ms to 10 s.[33−35] Due to the short time scale, fabrication of complex and winding configuration of microfluidic

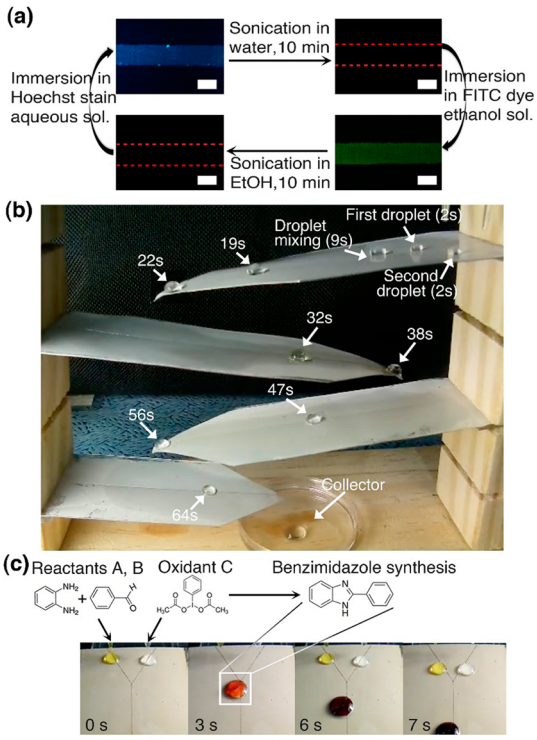

Figure 4. (a) Reusability test of the μ-OF device. Blue fluorescence that appeared on the omniphilic microchannel after immersion in the Hoechst solution disappeared by sonication in water. After immersion in an ethanol solution of FITC dye, green fluorescence appeared. The green fluorescence again disappeared by sonication in ethanol. This process can be repeated. The scale bar is 60 μm. (b) Multilayered μ-OF device for long-term and effective mixing [two water droplets (vol = 10 μL) were dropped from the two different microburets (slope angle = 5−10°)]. Movie frames were superimposed for droplets of water. (c) Model organic reaction between *o*-phenylenediamine and benzaldehyde to produce 2-arylbenzimidazole was performed on the μ-OF device. Yellow droplet (left) was a THF solution of *o*-phenylenediamine and benzaldehyde, and the colorless droplet (right) was a THF solution of iodobenzene diacetate.

channels is required to increase the running time. Fluidic channels with capability of more than 1 min running time can open a new direction of research. For example, studies of immune system compenents in blood such as T-cells and B-cells as well as cancer metastasis of circulating tumor cells require significantly long running time in fluidic channels. The μ-OF device has a great advantage for these purposes, which will be the future direction of our research. The extended running time by the multilayered μ-OF configurations is also expected to be beneficial for development of complex mixing strategies such as A + B → C for 20 s reaction and C + D → E for additional 20 s and then E + F → G, and so forth. Solvent evaporation can be a major problem as the μ-OF device is an open system. Each solvent droplet (20 μL) was weighed before and after the operation in the μ-OF device for 60 s. The percent solvent loss (loss of solvent mass/initial solvent mass × 100, %) was negligible for all tested solvents: 0.33 ± 0.28% for water, 0.31 ± 0.26% for DMSO, 0.35 ± 0.31% for DMF, 0.87 ± 0.37% for hexadecane, 1.12 ± 0.39% for diesel oil, 3.1 ± 0.33% for xylene, 4.36 ± 0.62% for 2-propanol, 6.54 ± 0.97% for ethanol, 7.58 ± 0.79% for 1,2-dichloroethane, and 9.78 ± 0.86% for THF (Supporting Information Figure S7). When the time scale from seconds to a minute is considered in most microfluidic systems, the μ-OF device might not exhibit serious problems in evaporation-related issues.

Finally, the multilayered μ-OF device can be used as a platform for multiassays. For example, various types of assay surfaces such as glucose assay, pH assay, or protein assay surfaces can be installed into the multilayered μ-OF device. By simple replacement of the surface, one can easily establish a various assay platform, which will also be a future direction of our research.

Model Organic Reaction. Owing to the solvent compatibility differences between μ-OF and PDMS-based systems, chemical reactions can be performed in organic solvents such as THF using μ-OF devices. The synthesis of benzimidazoles was chosen as a model reaction. Benzimidazoles are important, useful building blocks in therapeutic agents, such as antiviral and anticancer agents.[36−38] Both an 8 μL THF solution droplet containing two reactants (*o*-phenyldiamine (400 mM) and benzaldehyde (400 mM)) and an 8 μL THF droplet containing an oxidant, iodobenzene diacetate (IBD) were introduced to the Y-patterned surface channels (Figure 4c). The mixture solution in the microreactor was analyzed by ^{1}H NMR to verify the product and reaction yield. The reaction yield was calculated using the following equation: ((initial amount of benzaldehyde) − (final amount of benzaldehyde))/(initial amount of benzaldehyde) × 100. The final benzaldehyde amount was determined by comparing the integration of the aldehyde peak (9.99 ppm, singlet) from benzaldehyde to the integration value of the methyl peak (1.89 ppm, singlet) from IBD and acetic acid. The two equivalent methyl groups in the IBD oxidant generated 2 equiv of acetic acid after the reaction, which results in a constant NMR integration value (Supporting Information Figure S8) that can be used as an internal standard. The μ-OF device reaction yield was 70.3% (IBD = 200 mM) after incubating for 10 min at room temperature. Interestingly, the reaction yield was higher than that of a typical bulk reaction using a vial without changing the reactant concentrations (vol = 4 mL, IBD = 200 mM). The reaction yield was 52.1% (Supporting Information Table S2). The enhanced reaction yield of the μ-OF device may result from the decreased diffusion path length within the droplet, which results in a rapid and homogeneous mixing.[34] This result indicates that the μ-OF device can be used as a promising new microreactor for organic and aqueous reactions. The flow

rate of the μ-OF device (10−20 μL/s) is higher than that for conventional droplet-based, 3D microfluidic systems (~0.2 μL/s),[33−35] which increases the suitability for applications requiring large sample volumes.

CONCLUSION

In conclusion, a bioinspired, surface-tension-confined microfluidic device, called a micro-omnifluidic device, was demonstrated. The spatially controlled modification of a textured TiO_2 surface *via* biomimetic silicification generated microlines with high surface energies. Movement and effective droplet mixing in these silicified microlines are precisely controlled in an energy-efficient manner using gravity. The introduction of a relatively large silicified square patch at the intersection of the Y-patterned microlines controls the droplet movement, including stopping and starting. The μ-OF device is compatible with nearly all organic solvents, which removes the limitation of conventional surface-tension-confined microfluidic devices that could not be applied to organic solvents. A μ-OF device was used as a microreactor for an organic synthesis. The μ-OF device has great potential as a pump-free microfluidic system for various applications.

METHODS

Materials. Dopamine hydrochloride, titanium(IV) isopropoxide (99.999%, trace metal basis), 2-dimethylaminoethanethiol hydrochloride (DMAET, 95%), tetramethyl orthosilicate (TMOS, 99+%), sodium phosphate dibasic (99%), sodium phosphate monobasic (99%), Trizma base (99.9%), Trizma hydrochloride (99%), 2-propanol (≥99.5%), dimethyl sulfoxide, tetrahydrofuran, and Fluorinert FC-70 were purchased from Sigma-Aldrich. ZonylFSE was purchased from Fluka. Toluene, 1,4-dioxane, chloroform, and *N*,*N*-dimethylformamide were purchased from Junsei (Japan). Ethanol and methanol were purchased from Merck (USA). Aluminum was purchased from Alfa-Aesar (USA). MIF-300 and AZ 5214E were purchased from AZ electronic materials (UK). PDMS microchannels were prepared according to the literature method using Sylgard 184 silicon elastomer (Dow Corning).

Fabrication of the Fluorinated, Textured TiO_2 Surface. The poly(dopamine) (pDA) was coated on the bare aluminum surfaces by immersing the surfaces in a dopamine hydrochloride solution (2 mg/mL, pH 8.5, 10 mM Tris buffer) for 16 h. Then, titanium(IV) isopropoxide solution (~20%) (the titanium isopropoxide solution was diluted five times using 2-propanol) was poured onto the pDA-coated Al surface and immediately spin-coated at 1000 rpm for 15 s, resulting in the immediate formation of TiO_2 on the surface (the spin-coating was carried out at room temperature and at relative humidity of 60%). The substrates were then immersed in an ethanol solution of 1% zonylFSE for 20 min to functionalize the surface with the perfluorophosphate surfactant.

Formation of the Mussel- and Diatom-Inspired Silicified Microline Patterns. Silicified microline patterns were generated on the fluorinated, textured TiO_2 surface by photolithography combined with silicification before photoresist development. The fluorinated, textured TiO_2 surface (7 cm × 3 cm) was spin-coated with a positive photoresist (AZ 5214) at 4000 rpm for 35 s. Then, the surface was exposed to UV light (365 nm, I-line) for 30 s through a photomask and was subsequently developed for 50 s in a developer solution (MIF-300). The resulting surface was immersed in a dopamine solution (10 mM, 10 mL, pH 8.5) for 45 min at room temperature. After that, Tris buffer solution of DMAET (10 mM, 10 mL) was added, and surface functionalization was further performed for another 5 h at room temperature. The resulting surface was washed with deionized water and dried under a stream of nitrogen gas. Monosilicic acid was formed by stirring a 1 mM HCl solution of TMOS (100 mM) for 15 min at room temperature, and the solution of monosilicic acid (20 mL) was added to a 100 mM aqueous phosphate buffer (pH 6.0, 20 mL) containing the DMAET-modified surface. After 1 h incubation, the surface was washed with deionized water and dried under a stream of nitrogen. Finally, the remaining photoresist was removed by immersing the surface in acetone for 10 s.

Measurement of the Forces. The gravitational force and the adhesion force can be mathematically described by the relation of $F_{grav} = mg \sin\theta$ and $F_{adh} = \gamma_L D(1 + \cos\alpha)$, respectively, where m is the mass of the liquid droplet, g is the gravitational acceleration (9.81 m/s^2), and θ is the surface tilting angle (*i.e.*, the slope angle); γ_L is the surface tension of the liquid droplet, D is the perimeter length of the silicified omniphilic microchannel on the liquid/surface/air three-phase contact lines, and α is the static contact angle of the liquid droplet. The value of m was calculated by multiplying the known volume of the liquid droplet by the density. The value of θ was measured through a computer program "Arduino" (Italy) which operated the HS-475HB standard deluxe servo motor (Hitec, Korea) tilting the angle stage. The value of α was measured with a Phoenix 300 goniometer (Surface Electro Optics Co., Ltd., Korea).

Characterization. Static contact angles were measured with a Phoenix 300 goniometer (Surface Electro Optics Co., Ltd., Korea). Static water contact angles were measured at three different locations on each sample, and the average values are reported. Surface morphology was monitored by field emission SEM (S-4800, Hitachi). XPS was performed with an ESCA 2000 (Thermo VG Scientific, England) with a monochromatic twin X-ray source (Mg/Al target). ToF-SIMS measurements were taken using a ToF-SIMS Vinstrument (ION-TOF GmbH). Bi^{3+} ions with 25 kV were focused to achieve approximately 3 μm spatial resolution. Both positive and negative image data were obtained at an area of 500 × 500 μm^2 with 150 ms cycle time, and the PIDD (primary ion dose density) for analysis was 5.0 × 10^{11} ions/cm^2 to ensure static SIMS conditions. During data acquisition, low-energy electron flooding was used for charge compensation. For mass calibration, the CF^+ peak was used for positive data and the SiO_2^- peak was used for negative data. ^{1}H NMR data were recorded on a FT AM 400 (400 MHz). Chemical shifts were quoted in parts per million (ppm) referenced to the appropriate solvent peak or 0.0 ppm for tetramethylsilane. The thickness of the lubricating film (3 M Fluorinert FC-70) was measured using a confocal microscope (LSM 510 META microscope ,Carl Zeiss, Germany). The fluorinated TiO_2 surface (third step, Figure 1a) was contacted by a 10 μL droplet of doxorubicin (Dox) solution (0.2 mg/mL, in ethanol) and blown by N_2 gas, resulting in the surface adsorption of Dox molecules (λ_{exc} = 480 nm, λ_{em} = 580 nm). The Dox deposition is going to be the underneath fluorescent layer upon FC-70 application. After the lubricant infusion of the surface, a 1.5 μL droplet of fluorescein sodium salt solution (λ_{exc} = 488 nm, λ_{em} = 520 nm) was added on top of the FC-70 layer surface. The height of the ground surface was first assigned by detecting the red fluorescence from the Dox on the ground surface and focusing the image. Then, *Z*-stacking analysis from the ground height with the interval of 1.1 μm was performed. Green fluorescence from the fluorescein solution on the lubricating film was detected on each layer of the *Z*-stack.

Conflict of Interest: The authors declare no competing financial interest.

Acknowledgment. This work is supported from National Science Foundation of S. Korea: Midcareer Scientist Program (2014-002855) and The Ministry of Knowledge and Economy (World Premier Materials Program).

Supporting Information Available: Surface morphology by atomic force microscopy, contact angle measurement, stability test in organic solvents, ^{1}H NMR characterization, reaction yield at different conditions. This material is available free of charge *via* the Internet at http://pubs.acs.org.

REFERENCES AND NOTES

1. Whitesides, G. M. The Origins and the Future of Microfluidics. *Nature* **2006**, *442*, 368–373.
2. Roach, L. S.; Song, H.; Ismagilov, R. F. Controlling Nonspecific Protein Adsorption in a Plug-Based Microfluidic System by Controlling Interfacial Chemistry Using Fluorous-Phase Surfactants. *Anal. Chem.* **2005**, *77*, 785–796.
3. Mazutis, L.; Gilbert, J.; Ung, W. L.; Weitz, D. A.; Griffiths, A. D.; Heyman, J. A. Single-Cell Analysis and Sorting Using Droplet-Based Microfluidics. *Nat. Protoc.* **2013**, *8*, 870–891.
4. Juul, S.; Nielsen, C. J. F.; Labouriau, R.; Roy, A.; Tesauro, C.; Jensen, P. W.; Harmsen, C.; Kristoffersen, E. L.; Chiu, Y.-L.; Frøhlich, R.; *et al.* Droplet Microfluidics Platform for Highly Sensitive and Quantitative Detection of Malaria-Causing Plasmodium Parasites Based on Enzyme Activity Measurement. *ACS Nano* **2012**, *6*, 10676–10683.
5. Sheng, W.; Chen, T.; Tan, W.; Fan, Z. H. Multivalent DNA Nanospheres for Enhanced Capture of Cancer Cells in Microfluidic Devices. *ACS Nano* **2013**, *7*, 7067–7076.
6. Nisisako, T.; Torii, T.; Takahashi, T.; Takizawa, Y. Synthesis of Monodisperse Bicolored Janus Particles with Electrical Anisotropy Using a Microfluidic Co-Flow System. *Adv. Mater.* **2006**, *18*, 1152–1156.
7. Shum, H. C.; Abate, A. R.; Lee, D.; Studart, A. R.; Wang, B.; Chen, C.-H.; Thiele, J.; Shah, R. K.; Krummel, A.; Weitz, D. A. Droplet Microfluidics for Fabrication of Non-spherical Particles. *Macromol. Rapid Commun.* **2010**, *31*, 108–118.
8. Dittrich, P. S.; Manz, A. Lab-on-a-Chip: Microfluidics in Drug Discovery. *Nat. Rev. Drug Discovery* **2006**, *5*, 210–218.
9. Huh, D.; Matthews, B. D.; Mammoto, A.; Montoya-Zavala, M.; Hsin, H. Y.; Ingber, D. E. Reconstituting Organ-Level Lung Functions on a Chip. *Science* **2010**, *328*, 1662–1668.
10. Huh, D.; Torisawa, Y.-S.; Hamilton, G. A.; Kim, H. J.; Ingber, D. E. Microengineered Physiological Biomimicry: Organs-on-Chips. *Lab Chip* **2012**, *12*, 2156–2164.
11. Kastrup, C. J.; Nahrendorf, M.; Figueiredo, J. L.; Lee, H.; Kambhampati, S.; Lee, T.; Cho, S.-W.; Gorbatov, R.; Iwamoto, Y.; Dang, T. T.; *et al.* Painting Blood Vessels and Atherosclerotic Plaques with an Adhesive Drug Depot. *Proc. Natl. Acad. Sci. U.S.A.* **2012**, *109*, 21444–21449.
12. Lee, J. N.; Park, C.; Whitesides, G. M. Solvent Compatibility of Poly(dimethylsiloxane)-Based Microfluidic Devices. *Anal. Chem.* **2003**, *75*, 6544–6554.
13. You, I.; Yun, N.; Lee, H. Surface-Tension-Confined Microfluidics and Their Applications. *ChemPhysChem* **2013**, *14*, 471–481.
14. Schilling, K. M.; Lepore, A. L.; Kurian, J. A.; Martinez, A. W. Fully Enclosed Microfluidic Paper-Based Analytical Devices. *Anal. Chem.* **2012**, *84*, 1579–1585.
15. Carrilho, E.; Martinez, A. W.; Whitesides, G. M. Understanding Wax Printing: A Simple Micropatterning Process for Paper-Based Microfluidics. *Anal. Chem.* **2009**, *81*, 7091–7095.
16. Abe, K.; Kotera, K.; Suzuki, K.; Citterio, D. Inkjet-Printed Paperfluidic Immuno-Chemical Sensing Device. *Anal. Bioanal. Chem.* **2010**, *398*, 885–893.
17. Ishii, D.; Shimomura, M. Invisible Gates for Moving Water Droplets: Adhesive Force Gradients on a Biomimetic Superhydrophobic Surface. *Chem. Mater.* **2013**, *25*, 509–513.
18. Lee, H.; Dellatore, S. M.; Miller, W. M.; Messersmith, P. B. Mussel-Inspired Surface Chemistry for Multifunctional Coatings. *Science* **2007**, *318*, 426–430.
19. Lee, H.; Lee, B. P.; Messersmith, P. B. A Reversible Wet/Dry Adhesive Inspired by Mussels and Geckos. *Nature* **2007**, *448*, 338–341.
20. You, I.; Seo, Y. C.; Lee, H. Material-Independent Fabrication of Superhydrophobic Surfaces by Mussel-Inspired Polydopamine. *RSC Adv.* **2014**, *4*, 10330–10333.
21. Kang, S. M.; Hwang, N. S.; Yeom, J.; Park, S. Y.; Messersmith, P. B.; Choi, I. S.; Langer, R.; Anderson, D. G.; Lee, H. One-Step Multipurpose Surface Functionalization by Adhesive Catecholamine. *Adv. Funct. Mater.* **2012**, *22*, 2949–2955.
22. Kang, S. M.; Ryou, M. H.; Choi, J. W.; Lee, H. Mussel- and Diatom-Inspired Silica Coating on Separators Yields Improved Power and Safety in Li-Ion Batteries. *Chem. Mater.* **2012**, *24*, 3481–3485.
23. Wong, T.-S.; Kang, S. H.; Tang, S. K. Y.; Smythe, E. J.; Hatton, B. D.; Grinthal, A.; Aizenberg, J. Bioinspired Self-Repairing Slippery Surfaces with Pressure-Stable Omniphobicity. *Nature* **2011**, *477*, 443–447.
24. Vogel, N.; Belisle, R. A.; Hatton, B.; Wong, T.-S.; Aizenberg, J. Transparency and Damage Tolerance of Patternable Omniphobic Lubricated Surfaces Based on Inverse Colloidal Monolayers. *Nat. Commun.* **2013**, *4*, 2176.
25. Yao, X.; Hu, Y.; Grinthal, A.; Wong, T.-S.; Mahadevan, L.; Aizenberg, J. Adaptive Fluid-Infused Porous Films with Tunable Transparency and Wettability. *Nat. Mater.* **2013**, *12*, 529–534.
26. Gorb, E. V.; Baum, M. J.; Gorb, S. N. Development and Regeneration Ability of the Wax Coverage in *Nepenthes alata* Pitchers: A Cryo-SEM Approach. *Sci. Rep.* **2013**, *3*, 1–6.
27. Gorb, E. V.; Haas, K.; Henrich, A.; Enders, S.; Barbakadze, N.; Gorb, S. N. Composite Structure of the Crystalline Epicuticular Wax Layer of the Slippery Zone in the Pitchers of the Carnivorous Plant *Nepenthes alata* and Its Effect on Insect Attachment. *J. Exp. Biol.* **2005**, *208*, 4651–4662.
28. Gaume, L.; Perret, P.; Gorb, E.; Gorb, S.; Labat, J. J.; Rowe, N. How Do Plant Waxes Cause Flies to Slide? Experimental Tests of Wax-Based Trapping Mechanisms in Three Pitfall Carnivorous Plants. *Arthropod Struct. Dev.* **2004**, *33*, 103–111.
29. Schrader, M. E. Young−Dupre Revisited. *Langmuir* **1995**, *11*, 3585–3589.
30. Bangham, D. H.; Razouk, R. I. Adsorption and the Wettability of Solid Surfaces. *Trans. Faraday Soc.* **1937**, *33*, 1459–1463.
31. Butler, J. E.; Lü, E. P.; Navarro, P.; Christiansen, B. Comparative Studies on the Interaction of Proteins with a Polydimethylsiloxane Elastomer. *J. Mol. Recognit.* **1997**, *10*, 36–51.
32. Mukhopadhyay, R. When Microfluidic Devices Go Bad. How Does Fouling Occur in Microfluidic Devices, and What Can Be Done about It? *Anal. Chem.* **2005**, *77*, 429–432.
33. Song, H.; Tice, J. D.; Ismagilov, R. F. A Microfluidic System for Controlling Reaction Networks in Time. *Angew. Chem., Int. Ed.* **2013**, *42*, 767–772.
34. Teh, S. Y.; Lin, R.; Hung, L. H.; Lee, A. P. Droplet Microfluidics. *Lab Chip* **2006**, *8*, 198–220.
35. Song, H.; Chen, D. L.; Ismagilov, R. F. Reactions in Droplets in Microfluidic Channels. *Angew. Chem., Int. Ed.* **2006**, *45*, 7336–7356.
36. Roth, T.; Morningstar, M. L.; Boyer, P. L.; Hughes, S. H.; Buckheit, R. W.; Michejda, C. J. Synthesis and Biological Activity of Novel Nonnucleoside Inhibitors of HIV-1 Reverse Transcriptase. 2-Aryl-Substituted Benzimidazoles. *J. Med. Chem.* **1997**, *40*, 4199–4207.
37. Soderlind, K. J.; Gorodetsky, B.; Singh, A. K.; Bachur, N. R.; Miller, G. G.; Lown, J. W. Bis-benzimidazole Anticancer Agents: Targeting Human Tumour Helicases. *Anti-Cancer Drug Des.* **1999**, *14*, 19–25.
38. Du, L.-H.; Wang, Y.-G. A Rapid and Efficient Synthesis of Benzimidazoles Using Hypervalent Iodine as Oxidant. *Synthesis* **2007**, *5*, 675–678.